Model-Based Raman Simulations for Optimized Metrology in Nanosheet Transistor Devices

Stefan Schoeche*[a], Aron Cepler[b], Marjorie Cheng[b], Jander Cruz[a], Roy Koret[c], Lior Baltiansky[c], Maor Asher[c], Alexander Levy[c], Igor Turovets[c], and Daniel Schmidt[a]

[a]IBM Research, 257 Fuller Road, Albany, NY 12203, USA
[b]Nova Measuring Instruments Inc., 3342 Gateway Blvd, Fremont, CA 94538, USA
[c]Nova Ltd., 5 David Fikes St., Rehovot, 7632805, Israel

ABSTRACT

In-line Raman spectroscopy is an increasingly important metrology technique for nanosheet gate-all-around devices because it provides direct access to intrinsic material properties such as strain and SiGe composition through phonon mode analysis. While Raman peak positions primarily reflect these intrinsic properties, peak amplitudes are jointly governed by material properties and the three-dimensional (3D) device geometry. This amplitude-geometry relationship becomes critical in fully integrated 3D device structures, where multiple materials, deep canyons, and strong near-field localization can drive measurement sensitivity and signal crosstalk. Here, we demonstrate the value of model-based Raman (MBR) simulations to (i) attribute measured Raman contributions to specific regions of complex 3D structures, (ii) optimize wavelength and polarization configurations for targeted sensitivity (e.g., nanosheet channel versus substrate/fin), and (iii) mitigate interference between signals from different materials in the structure. Proof-of-concept results on $Si_{1-x}Ge_x$ line/space gratings and TiN-containing stacks, as well as case studies on integrated targets after high-k deposition and after pFET source/drain epitaxy, illustrate how MBR-guided configuration selection enhances sensitivity and supports robust in-line monitoring of strain and composition in nanosheet transistor technology.

Keywords: Raman spectroscopy, model-based simulation, nanosheet transistor, gate-all-around, strain metrology, in-line metrology

*Corresponding author: sschoeche@ibm.com

1. INTRODUCTION

Nanosheet gate-all-around transistors rely on strain-engineered channels and composition- and doping-controlled epitaxial source/drain regions to achieve higher carrier mobility and device performance [1]. Optimization of growth conditions for doped source/drain epitaxial material in fully integrated device structures is challenging due to nucleation from different Si facets and complicated gas flow characteristics in deep, narrow geometries [2]. Raman spectroscopy has proven effective for monitoring strain and composition in $Si/Si_{1-x}Ge_x$ nanosheet stacks via phonon mode analysis, providing a material fingerprint that is geometry-independent with respect to peak position [3]. However, understanding the peak amplitude information requires consideration of the local electromagnetic field distributions and the relative Raman scattering efficiencies from different regions of the device. Consequently, a model that accounts for the geometry of the sample and the intrinsic properties of all materials is required for full value extraction from the Raman measurement. This work focuses on model-based Raman simulations as a practical framework to optimize measurement configurations

and to interpret Raman signals from complex nanosheet structures. A variety of different sample systems from simple blanket films over line-space gratings to complex, fully integrated structures are discussed.

2. EXPERIMENTAL AND SIMULATION METHODS

2.1 In-line Raman spectroscopy

A typical Raman spectroscopy measurement on the $Si_{1-x}Ge_x$ alloy system is shown in Fig. 1 for blanket nanosheet stacks where the Ge concentration was adjusted between 25% and 50%. The expected contributions from the Ge-Ge mode, the Si-Ge mode and the Si-Si mode are indicated. Notably, the Si–Si mode region exhibits strong contributions from the unstrained silicon channels and the substrate, while the Si-Si mode attributed to the strained $Si_{1-x}Ge_x$ sheets is shifted which enables easy identification and characterization of the $Si_{1-x}Ge_x$ nanosheet strain and composition [3].

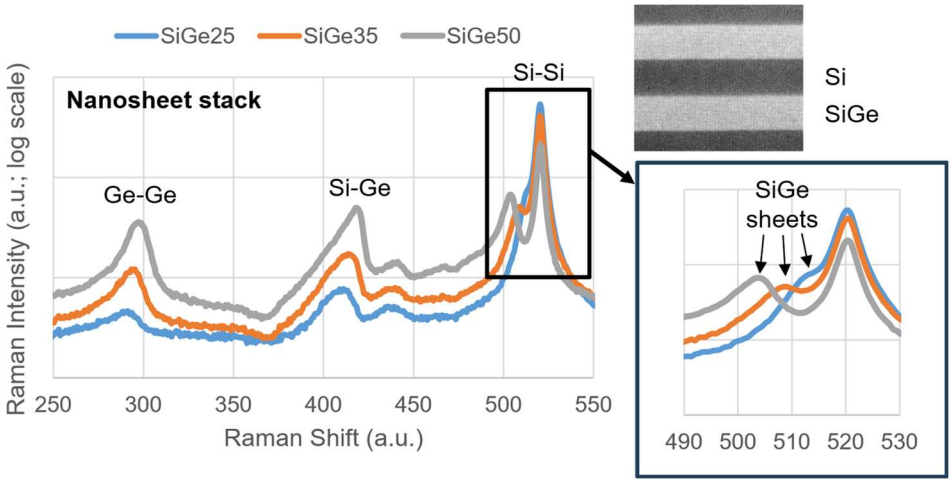

Fig. 1 In-line Raman spectroscopy data for a $Si/Si_{1-x}Ge_x$ nanosheet blanket film stack for Ge concentrations between 25% and 50% epitaxially grown on Si substrate. Expected phonon mode contributions assigned to the strained $Si_{1-x}Ge_x$ are indicated [3].

All experimental data in this study were acquired on a Nova Elipson in-line Raman tool. This tool is a multi-wavelength system with full continuous polarization control and a small spot size suitable for in-line characterization. The multi-wavelength capabilities are important because the Raman scattering efficiency in the $Si_{1-x}Ge_x$ alloy system depends on the excitation wavelengths [4]. Selection of the suitable excitation laser wavelength for a given percentage of Ge in the $Si_{1-x}Ge_x$ nanosheets maximizes the phonon mode amplitude and improves sensitivity to strain and composition. Continuous polarization control allows selection of the most suitable polarization state for any given Raman tensor symmetry and sample geometry. Commonly, input and detector polarization are either aligned parallel (Co-Pol) or the detector polarizer is rotated by 90° relative to the input polarization (Cross-Pol). Without simulation guidance, the optimal polarization configuration for a 3D structure must be determined empirically and may remain ambiguous due to (unknown) overlapping signal contributions.

2.2 Model-Based Raman simulations

The model-based Raman (MBR) simulations in this paper rigorously compute local electromagnetic field distributions and the global scattering efficiency for each component in a 3D sample based on the device geometry, optical constants, and the respective Raman tensors. These simulations calculate individual Raman

signal contributions in a 3D structure rather than relying on effective-medium or volume-averaged approximations. They can simulate multiple excitation wavelengths and polarization states, and near-field visualizations reveal the electric field hotspots that occur within the 3D structure. Optical critical dimension metrology (OCD) measurements can provide geometrical details and the material property input for these simulations.

3. RESULTS AND DISCUSSION

3.1 Proof-of-concept structures

As a proof-of-concept, MBR was applied to patterned $Si_{1-x}Ge_x$ line/space gratings and TiN blanket films of varying thickness deposited on thick SiO_2 films on Si substrates. The measured Raman data for $Si_{1-x}Ge_x$ line/space of varying line height is shown in Fig. 2a. The intensity of the Si-Si phonon mode of the $Si_{1-x}Ge_x$ lines increases with increasing line height, i.e., an increase in volume results in an increase in the measured Raman intensity. The respective MBR simulation results for the full stack as determined from OCD measurements are in excellent agreement with the experimentally determined Si-Si phonon mode amplitude (Fig. 2b).

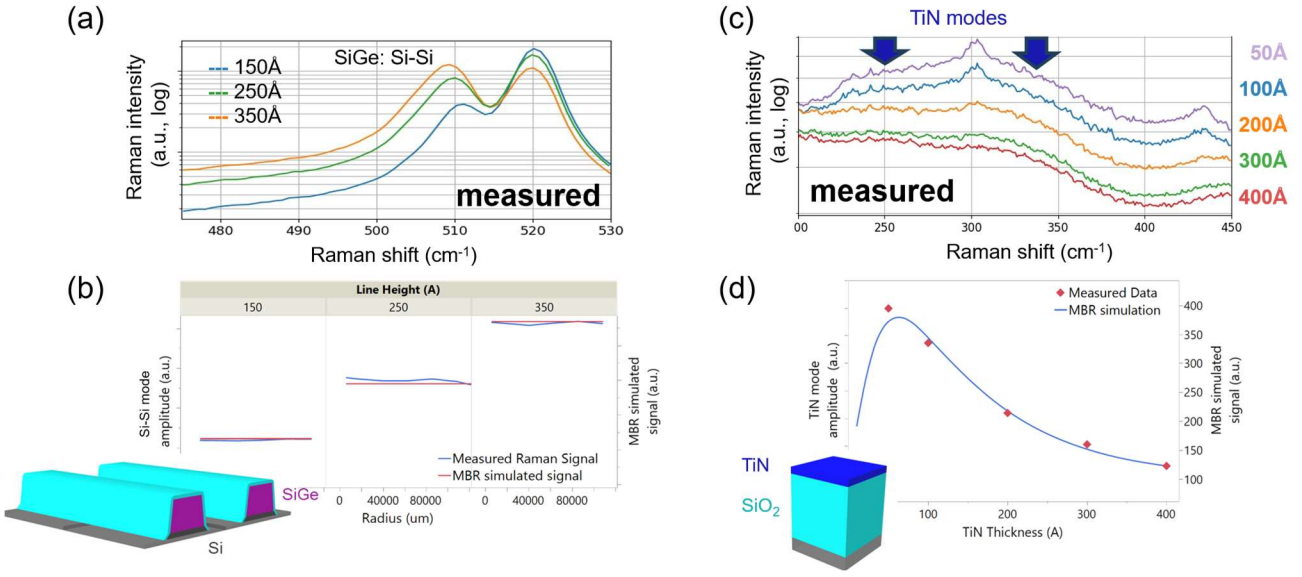

Fig. 2 (a) Measured Raman data for $Si_{1-x}Ge_x$ line/space gratings on Si with varying line height. (b) MBR simulations (red) in comparison to the measured Raman signal of the Si-Si mode (blue) for different line heights. (c) Measured Raman data for TiN films on thick SiO_2 layers on Si substrate for varying TiN film thickness. The expected location for TiN phonon modes is indicated by arrows. (d) Experimental TiN mode amplitude (symbols) in comparison with MBR simulated Raman signal (solid line) in dependence of TiN thickness.

Figure 2c shows measured Raman data for TiN blanket layers between 50Å and 400Å deposited on thick SiO_2 layers. Two phonon modes expected in the depicted spectral range are indicated by arrows in Fig. 2c. A decrease in the measured TiN phonon signal is observed with increasing film thickness, contradicting the intuitive assumption that an increase in film volume should result in increased Raman signal. In this sample system, optical field enhancement due to interference within the thick oxide is progressively damped as the TiN layer

thickness increases. MBR simulations predict the behavior correctly and can be used to predict optimum sample design to study thin layer properties on thick oxide films (Fig. 2d).

3.2 Post high-k deposition: nanosheet channel characterization

Raman measurements on fully integrated nanosheet transistor structures post high-k deposition provide access to the strain in the released nanosheet channels at a stage where channel dimensions and strain state are largely fixed. A typical in-line Raman measurement is shown in Fig. 3a. The expected contribution from the Ge-Ge, the Si-Ge, and the Si-Si associated with the source/drain epitaxial $Si_{1-x}Ge_x$ material are indicated. The strongest peak in the Raman spectrum is a convolution of two peaks associated with the Si nanosheets and the Si fin/substrate.

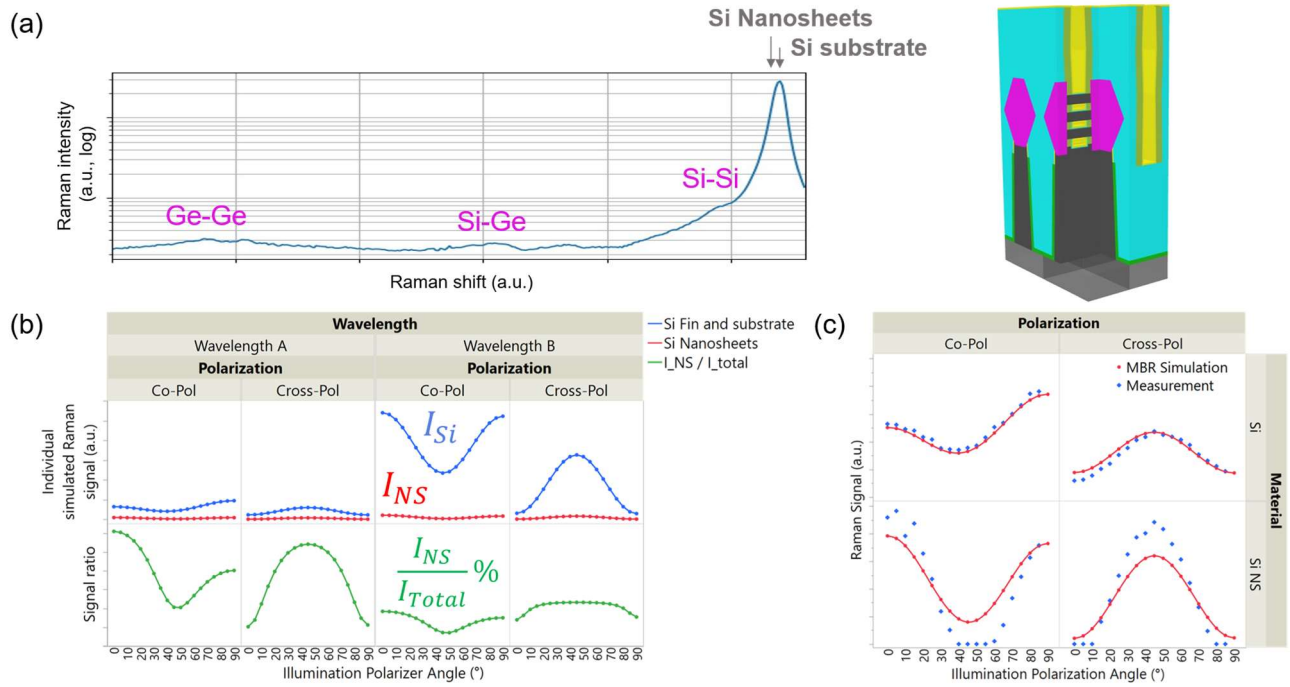

Fig. 3 (a) Typical in-line Raman spectrum of a fully integrated nanosheet transistor structure post high-k deposition. The 3D model of the sample structure as derived from OCD measurements is shown on the right. The typical contributions from the source/drain epitaxial $Si_{1-x}Ge_x$ material are indicated (magenta) as well as the Si nanosheet and fin/substrate contributions (grey). (b) MBR simulations for contributions from Si fin/substrate and the Si nanosheet channels in dependence of the illumination polarization for two different wavelengths (A shorter than B) and for Co-Pol and Cross-Pol polarization configurations. Absolute simulated Raman signal and the ratio between nanosheet contribution and the substrate/fin signal are shown. (c) Comparison of respective experimental and MBR simulated Raman signals measured with wavelength A.

MBR simulations can calculate the expected individual signal contributions of the Si nanosheet channel and the Si substrate/fin material for different polarization states and different excitation laser wavelengths. Figure 3b shows simulation results as a function of illumination polarization for two excitation wavelengths (A shorter than B), considering both Co-Pol and Cross-Pol configurations. Distinctly different signals for nanosheet and Si fin/substrate contributions for the two simulated excitation laser wavelengths are observed. At first glance, the Co-Pol configuration for wavelength B with 0° illumination polarizer angle appears the best possible measurement configuration since the nanosheet related signal is predicted to be highest here. However, this is

misleading without accounting for competing signal sources. Here, the strong fin/substrate signal will dwarf the nanosheet signal. The more suitable quantity to consider is the ratio of the nanosheet signal to the total Si signal intensity plotted in the bottom of Fig. 3b. Qualitatively, quite different behavior versus illumination polarizer angle is seen for the two wavelengths considered, with a broad dome-shaped feature in the Cross-Pol signal of wavelength A and a wide plateau for wavelength B. The strongest ratio between nanosheet signal and total Si signal is found for the Co-Pol configuration at 0° illumination polarizer orientation of wavelength A. The MBR simulations for different signal sources were instrumental here in finding the nominally best configuration to strain in the part of interest. The MBR simulation results were confirmed experimentally with excellent match between predicted results and measured Raman signal for both, the Si fin/substrate contribution and the Si nanosheets (Fig. 3c).

3.3 Influence of source/drain epitaxy on the nanosheet Si–Si phonon response

To understand the impact of the sample geometry on the channel Raman response, post-HK measurements were compared between fully integrated targets and targets without source/drain epitaxy. Significant changes in the raw data within the range of the Si–Si phonon mode were observed, including changes in peak center, amplitude, and asymmetry (Fig. 4a). This peak is a convolution of nanosheet and Si fin/substrate signal.

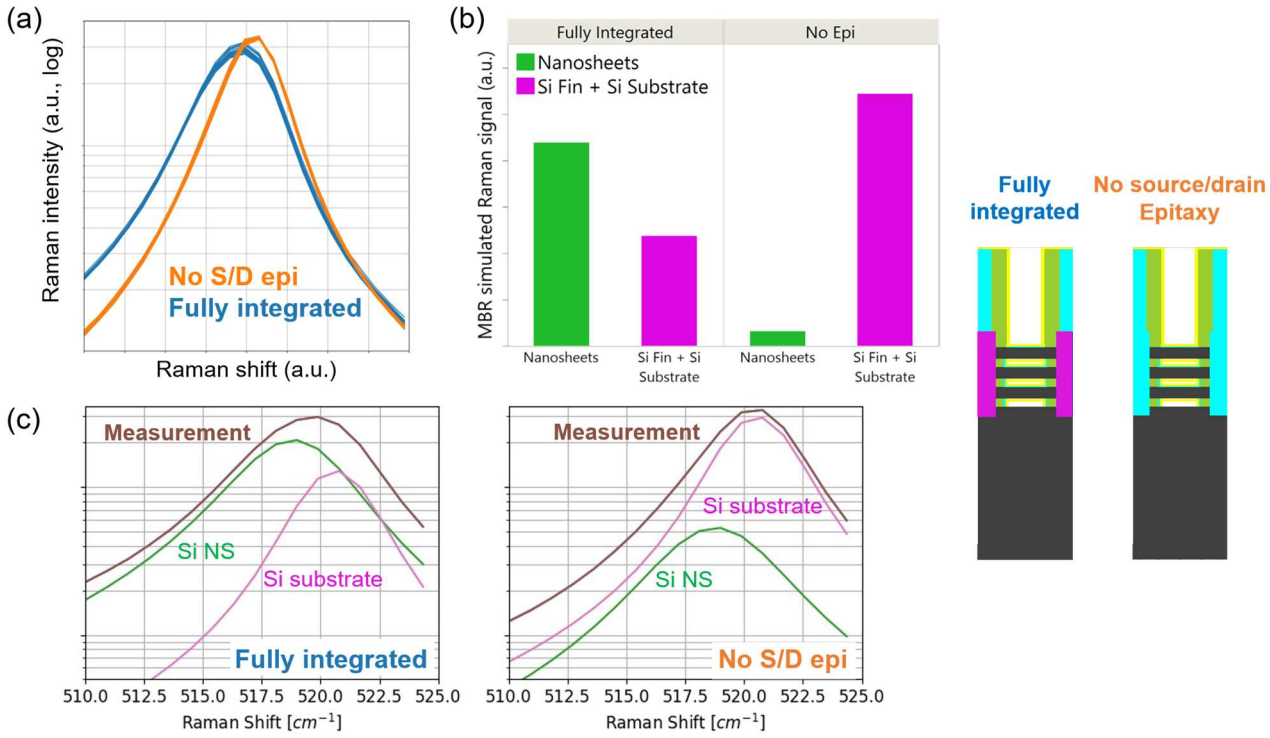

Fig. 4 (a) Experimental in-line Raman data comparison between measurements on a fully integrated target and a target with suppressed source/drain epitaxy post high-k deposition. (b) MBR simulated Raman signal for nanosheet and Si fin/substrate contributions for a fully integrated target and a target with suppressed source/drain epitaxy. (c) In-line Raman data (brown) and best-matching two-oscillator model for nanosheet (green) and Si fin/substrate contributions (magenta).

MBR simulations attribute these changes to altered optical field localization and modified relative contributions from nanosheets versus Si fin/substrate between the fully integrated target and target without source/drain epitaxy (Fig 4b). For the fully integrated target, a stronger nanosheet signal is predicted compared to the Si fin/substrate signal, while without source/drain epitaxial material, the nanosheet signal is much weaker than the Si fin/substrate signal. A peak-fitting analysis with a two-oscillator model to account for both contributions corroborates the MBR prediction. Note that possible correlation between the two peaks was carefully examined and does not impact peak fitting analysis results. In conclusion, for highest sensitivity to the nanosheet strain properties, measurements should be performed on fully integrated targets.

The near-field information extracted from the MBR simulations illustrates that in fully integrated structures the optical field localizes within the nanosheets, whereas in the absence of source/drain epitaxy the field may concentrate in the fin region below with reduced nanosheet localization (Fig. 5). These findings highlight that process-induced geometry and material changes can indirectly modify the measured Raman response even if intrinsic strain/composition remains unchanged, and that MBR is essential to separate intrinsic from optical/geometry-driven effects.

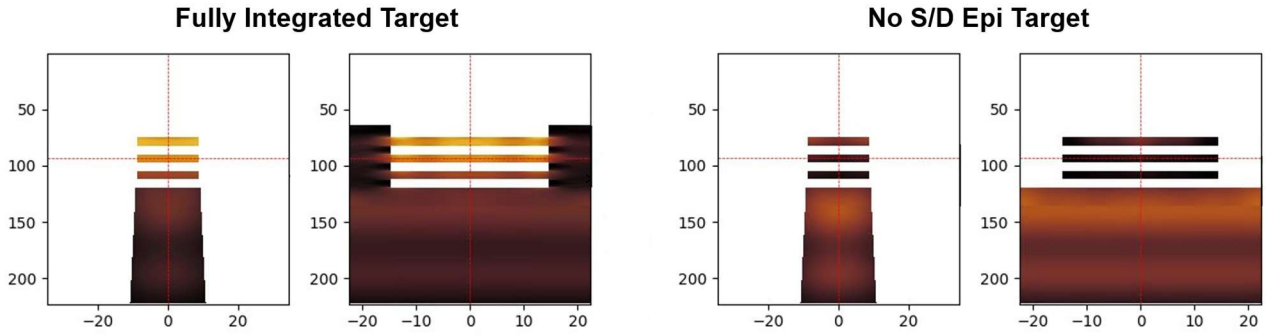

Fig. 5 MBR simulations of the near-field distribution in fully integrated target and targets with suppressed source/drain epitaxy. Cross-section over the fin and over the source/drain and nanosheet channels are shown. Identical color scales were used with brighter colors indicating a higher electric field strength.

3.4 Post pFET source/drain epitaxy: avoidance of interfering signals

The composition, strain, and dopant concentration in the epitaxially grown B-doped $Si_{1-x}Ge_x$ ($Si_{1-x}Ge_x$:B) pFET source/drain material will influence the performance and the yield of the nanosheet transistor devices. Optimized measurement configurations ensure highest sensitivity to the properties of interest without interference from other materials in the structure. At this process step, two components contain Ge: high percentage of Ge in the source/drain epitaxial material and lower percentage of Ge in the sacrificial SiGe nanosheet layers. While their Si-Si phonon modes are typically well separated, the weaker Si-Ge and Ge-Ge modes can overlap, and it can be challenging to deconvolute them in the peak fitting analysis. Access to all three modes is required to characterize strain, composition, and dopant concentrations from the in-line Raman data. Figure 6 shows the MBR simulated Raman signal for the epitaxial $Si_{1-x}Ge_x$:B source/drain material and the sacrificial $Si_{1-x}Ge_x$ nanosheets in dependence of polarization configurations. For all polarization configurations, the source/drain epitaxial material shows much higher Raman signals than for the sacrificial SiGe nanosheets. Thus, the nanosheet signal can either be neglected in first order since that process is typically well controlled and the contribution can be assumed to be stable wafer-to-wafer, or for highest accuracy, the

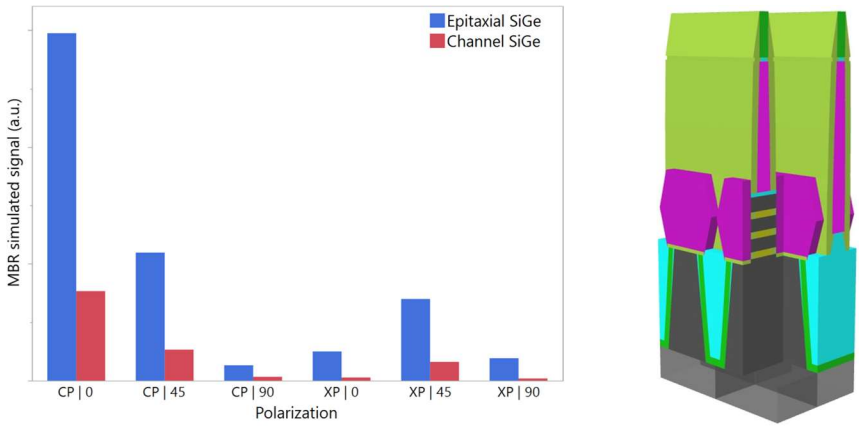

Fig. 6 MBR simulated Raman signal post pFET source/drain epitaxy for the epitaxial $Si_{1-x}Ge_x$:B source/drain material and the sacrificial $Si_{1-x}Ge_x$ nanosheets in dependence of polarization configurations (CP=Co-Pol, XP=Cross-Pol).

signal strength could be injected from previous measurements without the source/drain material being present yet.

The MBR simulations in Fig. 6 suggest that the highest signal for the source/drain epitaxial material can be expected for measurements in the Co-Pol configuration with illumination polarizer set to 0° (Co-Pol0). However, the measured Si-Ge peak amplitude was found to be highest for the Co-Pol configuration with illumination polarizer set to 90° (Co-Pol90, Fig. 7a). Importantly, the poly-Si in the dummy gate exhibits a Raman active phonon mode that overlaps with the Si-Ge mode of the epitaxial source/drain $Si_{1-x}Ge_x$ [5]. When the poly-Si of the dummy gate is included in the MBR simulations, a strong Raman signal is predicted for the Co-Pol90 configuration while a weak contribution is predicted for the Co-Pol0 configuration (Fig. 7b). In conclusion, the Co-Pol0 configuration is preferred to characterize the source/drain epitaxial material and the MBR simulations helped to identify the measurement configuration with minimum overlap from other components in the structure.

4. SUMMARY AND CONCLUSIONS

MBR simulations enable full value extractions from in-line Raman measurements by providing insights into the amplitude information for the complex Raman response in 3D structures. In a proof-of-concept study,

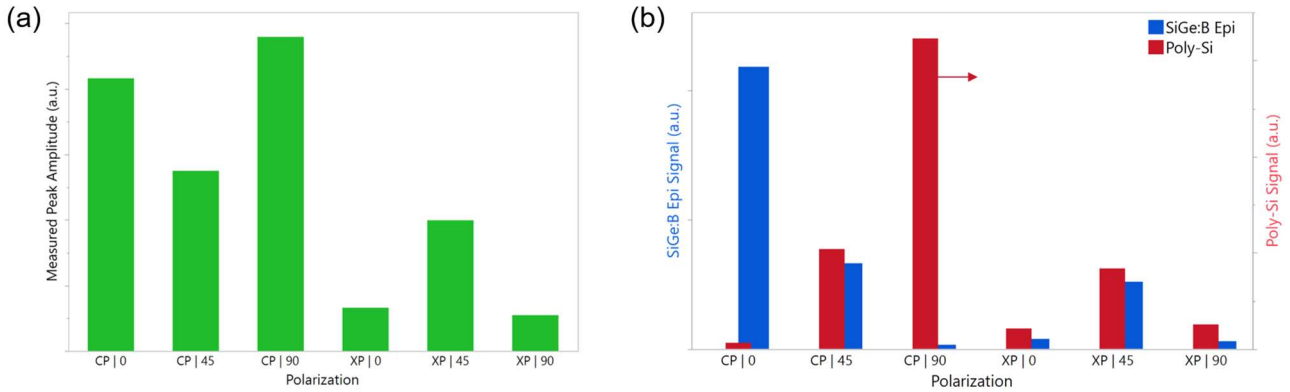

Fig. 7 (a) Measured in-line Raman signal of the Si-Ge phonon mode associated with the epitaxial source/drain $Si_{1-x}Ge_x$:B for different polarization configurations (CP=CoPol, XP=CrossPol). (b) MBR simulations for the Raman signal of the epitaxial source/drain $Si_{1-x}Ge_x$ and for the poly-Si in the dummy gate.

intuitive results were observed for simple line/space gratings and non-intuitive ones on TiN blanket thin films, both in the simulation and the experiment. For complex 3D structures, MBR provides optimum measurement configurations for maximum sensitivity, predicts the changing signal contributions for different structure modifications, for example, with and without epitaxial material, and provides guidance to avoid interfering signals. Near-field simulations visualize the origin of the Raman signal within the 3D structures. In conclusion, MBR simulations decompose complex signals for 3D structures and enable in-line Raman measurements with highest measurement selectivity to the properties of interest while minimizing interference from irrelevant contributions. More broadly, MBR establishes a physics-based framework to decouple intrinsic material properties from geometry- and optics-driven measurement artifacts in advanced 3D device metrology.

Acknowledgements

The authors would like to thank Chien-Fu Huang, Kishwar Mashooq, Trevor McDonough, Ruqiang Bao, Jun Liu (all IBM), Paul Isbester and Sarah Okada (both Nova Measuring Instruments) for support and fruitful discussions.

REFERENCES

1. Loubet, N. *et al.*, "Stacked nanosheet gate-all-around transistor to enable scaling beyond FinFET." 2017 symposium on VLSI technology. IEEE, pp. T230-T231 (2017).
2. H. Peng, Y. Yao, K. Shariar, J. Chen, D. Mafrici and K. Briggs, "Reducing Merged Silicon-Germanium (SiGe) Epitaxial Growth in FinFETs to Avoid Yield Loss," 2023 34th ASMC, pp. 1-5 (2023).
3. Schmidt, D., Durfee, C., Li, J., Loubet, N., Cepler, A., Neeman, L., Meir, N., Ofek, J., Oren, Y. and Fishman, D., "In-line Raman spectroscopy for gate-all-around nanosheet device manufacturing. ", Journal of Micro/Nanopatterning, Materials, and Metrology, *21*(2), pp.021203-021203 (2022).
4. Picco, A., Bonera, E., Grilli, E., Guzzi, M., Giarola, M., Mariotto, G., Chrastina, D. and Isella, G., "Raman efficiency in SiGe alloys". Phys. Rev. B—Condensed Matter and Materials Physics, *82*(11), p.115317 (2010).
5. Tallant, D.R., *et al.* "Characterization of polysilicon films by Raman spectroscopy and transmission electron microscopy: A comparative study." *MRS Online Proceedings Library (OPL)* 324, p. 255 (1993).